Eavesdropping Measurements for Applications in Office Environments at Low THz Frequencies

Tobias Doeker, *Graduate Student Member, IEEE*, Christoph Herold, *Graduate Student Member, IEEE*, Johannes M. Eckhardt, *Graduate Student Member, IEEE*, and Thomas Kürner, *Fellow, IEEE*

***Abstract*— Low terahertz (THz) frequencies are promising candidates for future wireless communication systems. Due to high path losses at those frequencies, highly directive antennas can be used to compensate the path losses thus making eavesdropping challenging. However, previous work has shown that eavesdropping is still possible even if antennas with pencil beams are used. In this article, eavesdropping possibilities are evaluated with respect to common objects in office environments–a coffee cup, a thermos, and a laptop–by investigating the scattering properties of these objects. For the coffee cup and the thermos, angle-independent reflection losses are given. The laptop has the lowest reflection losses of approximately 5 dB if it is placed to reflect the signal in a specular way. Furthermore, the results are analyzed in terms of secrecy capacity and blockage, revealing good eavesdropping opportunities when the thermos is used. If the object is placed outside of the line-of-sight path, the blockage drops down to zero. However, especially for the thermos the secrecy capacity is still below 0.8 in this case. For the other objects, a direct eavesdropping where Eve is directly oriented toward Alice results in a lower secrecy capacity in most of the cases.**

***Index Terms*— Blockage, coffee cup attack, eavesdropping, physical layer security, scattering properties, secrecy capacity, 300 GHz, THz communications.**

I. Introduction

THE low terahertz (THz) frequencies (0.1 – 1 THz) are envisioned for high data rate communications as there is a large available bandwidth. The IEEE 802.15.3d standard for high data rate communication [1] foresees wireless communication between 252 and 325 GHz. Envisioned use cases and scenarios such as data center communication, kiosk downloading, or wireless backhaul networks could also be a potential target for eavesdropping. Although the propagation at the low THz frequencies is challenging due to a high free space path loss (FSPL) and their susceptibility to weather effects such as water vapor absorption [2], [3], [4], the usage of high gain antennas and aligned point-to-point communication links can enable wireless THz communication [5], [6].

In theoretical work, these circumstances often lead to the assumption that communication links at low THz frequencies are inherently secure [7], [8]. Work at lower frequencies, however, has shown that eavesdropping is still possible [9]. In addition, previous work showed a strong influence of reflections of common scenario features such as door frames or TV-screens [10], suggesting that the assumption of inherently secure communication links has to be carefully evaluated. Apart from structures and fixed features of a scenario, movable objects can have an impact on the propagation, too, and could be used or placed specifically for attacks by skilled, potential eavesdroppers.

The effects of reflections and scattering at THz frequencies have been studied in a variety of research contributions. In earlier works, a focus on basic properties such as surface roughness or material parameters [11], [12], [13] can often be observed. In recent years, the focus has shifted more toward application specific measurements: the influence of a cylinder and a metal plate as scattering objects in and close to the line-of-sight (LOS) path have been studied at 100, 200, and 400 GHz by Ma et al. [14]. The effect of side lobes has been reduced by the usage of lenses. The results show however that pencil-beam-like communication links do not guarantee physical layer security. Similar experiments have been conducted previously at 60 GHz showing a decrease of physical layer security due to the placement of scattering objects [15]. Besides that [16], [17] even showed that atmospheric conditions can impact and impair the physical layer security of a THz communication link. In addition to eavesdropping, recent investigations are also focused on possibilities of jamming attacks [18].

As the communication at THz frequencies has significantly matured during the recent years [5], [19], the measurement campaign that is presented in this article focuses on objects that can be found in typical communication scenarios such as the meeting room scenario from [10]. The measurement setup therefore focuses on a system-level view rather than fundamental measurements using dedicated reflectors or specifically designed shapes. Therefore, in contrast to [14], no lenses have been used to include the effect of side lobes in combination with scattering objects. The measurement campaign hence complements the results from [10] by investigating the effect of scatterers at different distances, complex shapes as well

Manuscript received 30 September 2022; revised 20 December 2022; accepted 22 December 2022. Date of publication 20 January 2023; date of current version 5 June 2023. This work was supported by the German Research Foundation (DFG) "Meteracom—Metrology for THz Communications" under Grant FOR 2863. This article is an extended version from the *International Workshop on Mobile THz Systems*, Duisburg, Germany, July 4–6 2022. *(Corresponding author: Tobias Doeker.)*

The authors are with the Institute for Communications Technology, Technische Universität Braunschweig, 38106 Braunschweig, Germany (e-mail: doeker@ifn.ing.tu-bs.de; herold@ifn.ing.tu-bs.de; eckhardt@ifn.ing.tu-bs.de; kuerner@ifn.ing.tu-bs.de).

Color versions of one or more figures in this article are available at https://doi.org/10.1109/TMTT.2023.3236018.

Digital Object Identifier 10.1109/TMTT.2023.3236018

as the influence of different materials, orientations, and temperatures. In doing so, the contribution of the article extends the findings in [20] by analyzing the measurement campaign with a more in-depth view. Furthermore, different aspects and further objects are analyzed in this article compared to [20]. The contribution of this publication is twofold based on the comprehensive measurement campaign.

1) The results are analyzed with respect to scattering properties in terms of reflection losses for the different objects. The reflection losses are evaluated for different angles and characteristics like temperature and orientations of the object.
2) The results are used to calculate the secrecy capacity and blockage in the different scenarios to investigate the eavesdropping opportunities using the different scattering objects.

The following sections are structured as follows. The used measurement equipment and the measurement setup are described in Section II, followed by the analysis of the scattering properties in Section III. The secrecy capacity is evaluated in Section IV, and finally the results are concluded in Section V.

II. Measurement Methodology

To investigate eavesdropping possibilities, measurements were performed in a conference room scenario. The setup was chosen to emulate a typical conference situation. All investigations in this article are based on the received power of Eve and Bob. To measure the received power, a channel sounder was used. The channel sounder and the measurement setup are explained in detail in Sections II-A and II-B.

A. Measurement Equipment

The channel sounder that was used measures the channel impulse response (CIR) in the time domain by cyclic correlation of a transmitted and received signal. As a pseudorandom noise (PN) sequence offers good correlation properties, it is used as a test signal and it is generated by means of the base clock of 9.22 GHz in the PN sequence generator (PNG). The signal in the intermediate frequency (IF) band has a bandwidth of approximately 8 GHz and a center frequency of 9.2 GHz. Within the transmitter (TX) frequency extender, the IF signal is upconverted to a center frequency of 304.2 GHz by a multiple of the base clock and radiated with a power of −23.7 dBm. Following the same approach, the received radio frequency (RF) signal is downconverted within the receiver (RX) frequency extender. In the end, the IF signal is sampled in-phase and quadrature with analog-to-digital converters (ADCs) within the RX ultra wide-band (UWB) module with a subsampling of 128 and processed on the control laptop [21]. Generally, the channel sounder can perform multiple input multiple output (MIMO) measurements up to a configuration of four TX and four RX. In this work, one TX and two RX were used. According to common practice in eavesdropping investigations, the TX is called “Alice,” the first RX–which is the desired communication partner of Alice–is called “Bob,” and the second RX–which is the eavesdropper–is called “Eve.”

TABLE I
Technical Parameters of the Channel Sounder [21]

Parameter	Value
Clock frequency	9.22 GHz
Bandwidth	8 GHz
Chip duration	108.5 ps
M-sequence order	12
Sequence length	4095
Sequence duration	444.14 ns
Subsampling factor	128
Acquisition time for one CIR	56.9 µs
Measurement rate	17 590 CIR/s
Center frequency	304.2 GHz

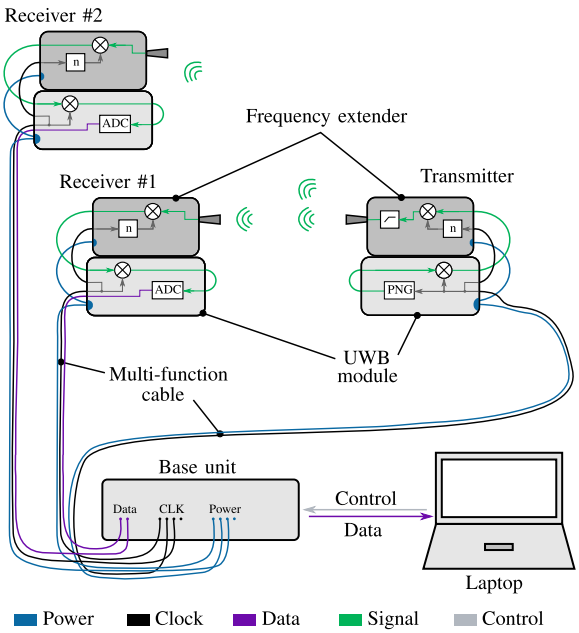

Fig. 1. Schematic block diagram of the channel sounder.

For all measurements, standard gain horn antennas with an antenna gain of $G_{\mathrm{TX,max,dB}} = G_{\mathrm{RX,max,dB}} = 26.4$ dBi and a half power beamwidth (HPBW) of 8.5° were used with vertical polarization. A schematic block diagram and a partial illustration of the channel sounder is shown in Figs. 1 and 2, respectively. A summary of the parameters of the channel sounder is given in Table I.

The PNG and the ADCs wake up in an arbitrary state that causes an arbitrary additional delay in the CIR every time the channel sounder is switched on. Measuring also relative values, the channel sounder has to be calibrated with respect to the amplitude and to the delay of the CIR with a back-to-back (B2B) calibration. By measuring the amplitude and the delay of known waveguides, a correction term can be calculated following the procedures described in [22] and [23], respectively. However, due to IQ-imbalances, the measurements are affected by an inaccuracy of up to ±2 dB but the calibration of the imbalances is an ongoing topic [24].

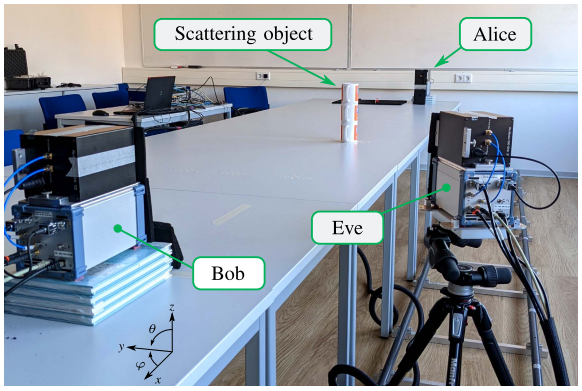

Fig. 2. Partial illustration of the measurement setup (based on [20]).

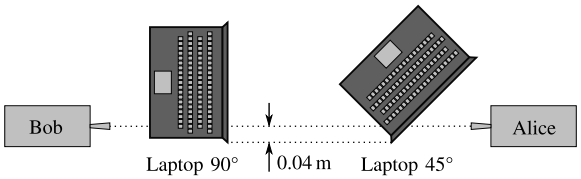

Fig. 3. Schematic top down view of the laptop orientation.

B. Measurement Setup

The whole measurement setup is placed in a conference room. Due to the post-processing and reference measurements, the influences of the room itself are compensated during the evaluation of the measurement data. Therefore, the CIR with the investigated object are compared to the CIR of the reference measurement without the object. By doing so, the multipath components (MPCs) caused by the investigated object can clearly be detected due to the different delay. Only these MPCs are chosen and further investigated. Alice and Bob are placed on tables, emulating communication partners in a typical office scenario like, e.g., laptop-to-laptop or laptop-to-projector configuration. The LOS path between Alice and Bob is parallel to the edge of the tables and marks the zero reference of the y-axis, whereas the edge of the horn antenna of Alice marks the zero reference of the x-axis. Therefore, Alice is placed at $x_{\text{Alice}} = 0$ m and $y_{\text{Alice}} = 0$ m with an azimuth angle of $\varphi_{\text{Alice}} = 0°$. Bob is placed at $x_{\text{Bob}} = 4.5$ m and $y_{\text{Bob}} = 0$ m with an azimuth angle of $\varphi_{\text{Bob}} = 180°$. During the measurements, neither the position nor the orientation of Alice and Bob are changed. Furthermore, the elevation angles of Alice, Bob, and Eve are not changed and remain at $\theta_{\text{Alice}} = \theta_{\text{Bob}} = \theta_{\text{Eve}} = 90°$ (only azimuth plane).

The position of Eve is fixed in the y-position at $y_{\text{Eve}} = -0.55$ m with Eve being moved along the x-axis for the different steps of the measurement. Therefore, Eve is placed on a tripod that is mounted on a platform of a rail system enabling an axial movement (see Fig. 2). Starting from $x_{\text{Eve,start}} = 0$ m up to $x_{\text{Eve,end}} = 4.5$ m, Eve is placed at ten different positions with a distance of $\Delta x_{\text{Eve,dist}} = 0.5$ m each. The height of the tripod is fixed so that Eve is on the same height as Alice and Bob. As mentioned before, the elevation angle of Eve is fixed but the azimuth angle is changed according to the position of Eve and the position of the scattering object as described below. The main lobe of the antenna of Eve is always oriented toward the direction of the center of the scattering object. This leads to azimuth angles in the range of $\varphi_{\text{Eve}} = [8; 170]°$. At larger x-positions of Eve, the Alice-Eve LOS path becomes dominant compared to the reflected path by means of the scattering object. However, due to the different delay, the components are separated in the CIR and can be identified clearly. It should be noted that only the values caused by the reflection at the scattering object are considered for the evaluation of the data.

To investigate the eavesdropping opportunities, three different scattering objects which are typical for a conference room scenario–namely a ceramic coffee cup, a thermos, and an open laptop–were used. In addition, the open laptop was used in two different configurations: 1) the surface of the opened laptop is perpendicular to the LOS path between Alice and Bob (called "Laptop 90°") and 2) with an angle of 45° with respect to the LOS path between Alice and Bob (called "Laptop 45°"). The different configurations are shown in a schematic top down view in Fig. 3.

The objects were placed at nine different positions grouped into three segments with the same x-position each with three different y-positions. The three segments are placed at $x_{\text{scat}} = [1.5; 2.5; 3.5]$ m. For each segment the object is placed at three different y-positions: first at $y_{\text{scat}} = 0$ m, i.e., in the LOS path; second at the corresponding positions where the object receives the signal from Alice with an angle of departure (AOD) of 4°; and finally at the corresponding positions where the object receives the signal from Alice with an AOD of 7°. A schematic top view including, among others, the different positions of the scattering object is shown in Fig. 4. It should be noted that the coffee cup and the thermos were placed centrically at the determined positions. The coffee cup has a diameter of approximately 8.5 cm and the thermos has a diameter of approximately 7.5 cm. The position of the laptop was arranged in such a way that the edge of the laptop is as far away from the determined positions as the coffee cup and the thermos (i.e., the radius of the coffee cup and the thermos). Therefore, the edge of the laptop had a distance of -0.04 m in y-direction to the determined positions as illustrated in Fig. 3 where the marked LOS path corresponds to the scattering positions at $y_{\text{scat}} = 0$ m.

Besides the measurements with the scattering objects, the same measurement is repeated without the scattering objects. This reference measurement is performed with the same setup, i.e., the same positions and angle of arrivals (AOAs) of Eve (Alice and Bob are fixed anyway) to give information about the MPCs which are caused by the environment. In addition, one reference measurement is conducted where Eve is aligned directly to Alice and not to the position of the scattering object.

III. Scattering Properties

In this section, the general reflection and scattering properties of the used objects are characterized. Furthermore, some special effects like the changes in characteristics due to the temperature or the orientation of the object are investigated. For calculating the reflection loss $L_{\text{refl},\alpha,\text{dB}}$ where α denotes the investigated object, only the MPC caused by the reflection at

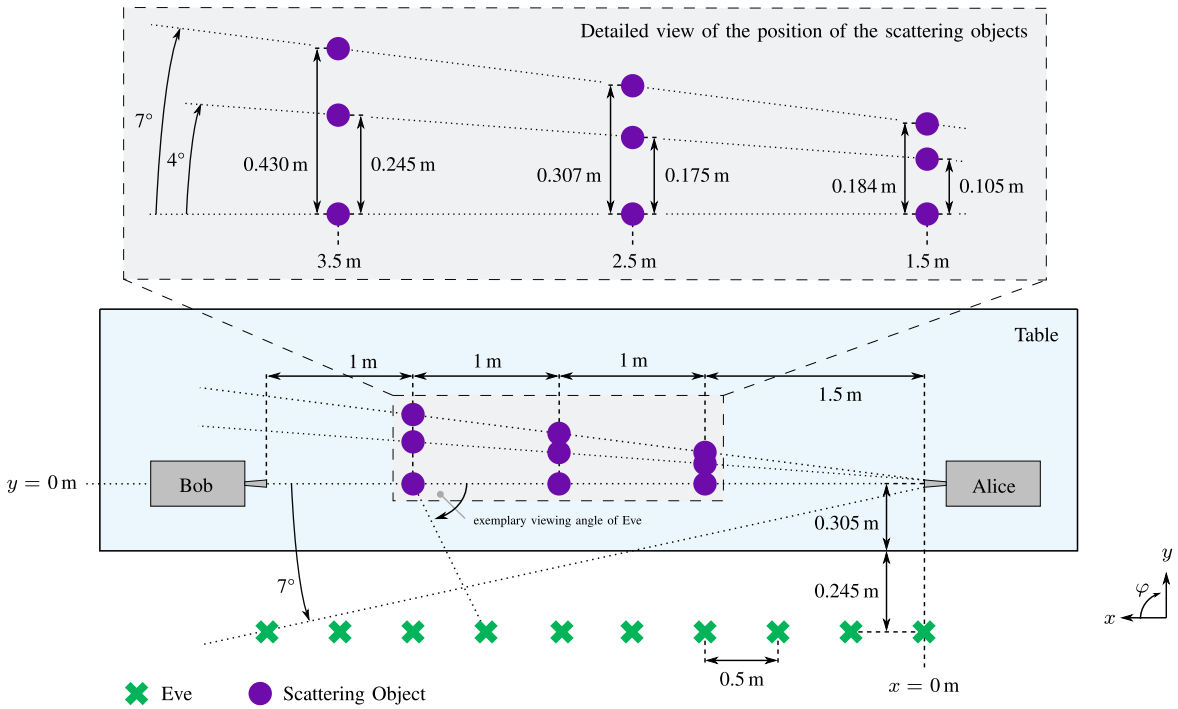

Fig. 4. Schematic top down view of the measurement setup in the conference room (based on [20]).

the investigated scattering object is evaluated. It can be identified using the reference measurement without the scattering object and the expected delay due to the physical setup. The FSPL can be calculated considering the delay τ_α by

$$L_{\mathrm{FSPL},\alpha,\mathrm{dB}} = 20 \cdot \log_{10}(4\pi f \cdot \tau_\alpha). \tag{1}$$

The reflection loss is then calculated as the difference between the measured path loss (PL) $L_{\mathrm{meas},\alpha,\mathrm{dB}}$ and the theoretical FSPL due to the delay

$$L_{\mathrm{refl},\alpha,\mathrm{dB}} = L_{\mathrm{meas},\alpha,\mathrm{dB}} - L_{\mathrm{FSPL},\alpha,\mathrm{dB}}. \tag{2}$$

Here, (2) holds for measurements with omni-directional antennas with an antenna gain of 0 dBi but during this measurement highly directive antennas were used. However, the antenna gain of the used antennas is compensated with respect to the antenna gain of the main lobe $G_{\mathrm{TX,max,dB}}$ and $G_{\mathrm{RX,max,dB}}$ in the post-processing so that (2) holds for these measurements in direction of the main lobe of the directional antennas, too. As the amplitude of the MPC is underestimated if the AOD or AOA does not correspond to the main lobe of the antenna ($\varphi = 0°$), the difference between the antenna gain of the main lobe and the antenna gain in the specific direction has to be added. In the discussed scenario, Eve is always oriented toward the center of the scattering object and therefore the AOA always falls together with the direction of the main lobe. However, the scattering object is not always placed in the main radiation direction of Alice so that the difference of the antenna gain

$$G_{\mathrm{diff,dB}} = G_{\mathrm{TX,max,dB}} - G_{\mathrm{TX,dB}}(\varphi_{\mathrm{AOD}}) \tag{3}$$

where φ_{AOD} is 4° and 7°, respectively, has to be considered resulting in

$$L_{\mathrm{refl},\alpha,\mathrm{dB}} = L_{\mathrm{meas},\alpha,\mathrm{dB}} - L_{\mathrm{FSPL},\alpha,\mathrm{dB}} - G_{\mathrm{diff,dB}}. \tag{4}$$

As mentioned in the context of the measurement equipment, the maximum antenna gain here is $G_{\mathrm{TX,max,dB}} = 26.4$ dBi and for the different AODs the antenna gain is $G_{\mathrm{TX,dB}}(4°) = 23.98$ dBi and $G_{\mathrm{TX,dB}}(7°) = 18.68$ dBi.

A. General Characteristics

Due to the different positions of the scattering object and of Eve, each measurement gives the reflection loss of the object for a different viewing angle of Eve with respect to the incident wave, as exemplarily shown in Fig. 4. The results show that the scattering properties of the coffee cup and the thermos are better than the scattering properties of the laptop in most of the cases as can be seen in Fig. 5. The majority of the reflection losses in the considered angular range are within the range of [23; 28] dB and [16; 21] dB for the coffee cup and the thermos, respectively, whereas they are within the range of [34; 47] dB and [33; 40] dB for the Laptop 45° and Laptop 90°, respectively. The ranges are visualized in Fig. 6. However, the lowest reflection losses are measured for the Laptop 45° if the signal is received with a viewing angle close to 90°. This is further investigated in Section III-C.

With respect to the coffee cup and the thermos, the results additionally emphasize that the thermos reflects better than the coffee cup due to the metallic surface of the thermos. The reflection losses of the thermos are approximately 7 dB lower compared to the reflection losses of the coffee cup. In addition, the reflection losses for both, the coffee cup and the thermos, as well as the reflection losses for the Laptop 90° are limitedly spread and therefore there are nearly identical in a first-order approximation for all investigated angles. The difference between the lower and upper quartile is only 4 dB for the coffee cup and the thermos as well as 5.6 dB for the Laptop 90°. Therefore, the average value of 26.9 dB

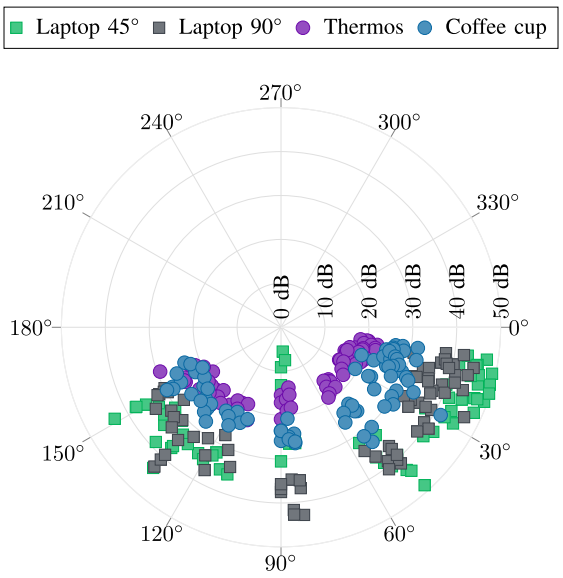

Fig. 5. Reflection losses for different viewing angles of Eve and different objects.

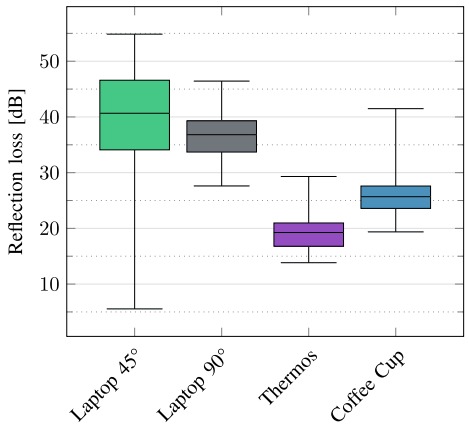

Fig. 6. Distribution of the reflection losses for different objects.

for the coffee cup, 19.8 dB for the thermos, and 37.5 dB for the Laptop 90° can be used as reflection losses that are independent of the viewing angle for simple models in the investigated angular range.

B. Temperature Characteristics

In the previous and in the following sections, the objects–more specifically the coffee cup and the thermos–were empty. To evaluate the difference of the scattering properties for different temperatures of the objects, they were filled with cold and hot water. For these measurements, Eve was fixed at $x_{\text{Eve}} = 2.5$ m and the scattering object was placed at all three y-positions for $x_{\text{scat}} = 2.5$ m. To differentiate the impact of the content itself, reference measurements with empty objects were performed at $y_{\text{scat}} = 0$ m and at $y_{\text{scat}} = 0.175$ m. For $y_{\text{scat}} = 0$ m, the difference in the transmission by evaluating the received power of Bob is also analyzed. The measurement results are post-processed to compensate the FSPL and the antenna gain resulting in the reflection and transmission loss.

With respect to the scattering properties, there are no differences neither between empty or full nor between cold or hot objects detectable. The reflection losses, summarized in Table II, are always in the same order of magnitude considering the tolerance of the measurement equipment. The same observations can be made for the transmission loss (summarized in Table III). The transmission loss is also always in the same order of magnitude.

TABLE II
REFLECTION LOSS

	Position y-axis	0 m	0.175 m	0.307 m
Coffee Cup	empty	24.18 dB	–	–
	cold	23.19 dB	25.97 dB	24.38 dB
	hot	23.27 dB	23.95 dB	22.61 dB
Thermos	empty	17.21 dB	16.00 dB	–
	cold	17.70 dB	16.27 dB	16.70 dB
	hot	17.92 dB	17.29 dB	16.10 dB

TABLE III
TRANSMISSION LOSS

	empty	cold	hot
Coffee Cup	11.72 dB	11.25 dB	11.99 dB
Thermos	13.22 dB	12.76 dB	10.52 dB

C. Orientation Characteristics

The reflection properties of the thermos are independent of the orientation of the thermos as the thermos is rotationally symmetric, i.e., the reflecting surface is always the same. On the other hand, the coffee cup has a handle. However, in most cases the reflecting surface is still the same because the coffee cup is also circular and the handle is mostly covered by the coffee cup, but for some orientations the reflecting surface might be different. Therefore, the difference of the reflection properties of the coffee cup are evaluated for different orientations. Eve was placed at $x_{\text{Eve}} = 2.5$ m and the coffee cup was placed at $x_{\text{scat}} = 2.5$ m and $y_{\text{scat}} = 0$ m as well as $y_{\text{scat}} = 0.307$ m. The handle was set starting at $\varphi_{\text{handle}} = 0°$ up to $\varphi_{\text{handle}} = 315°$ in 45° steps resulting in several different angles of the orientation of the handle with respect to the incident angle of the signal.

The measured values do not give any information about the orientation of the handle. The values are neither constant nor do they change in a particular way, they seem to be randomly distributed. Fig. 7 shows the measured values along with the average value. Except for a few values, the measured values lie within the accuracy of the channel sounder as the values are within the average value ±2 dB as visualized in Fig. 7. It should be noted that even the outliner at approximately 150° does not correspond to an appropriate configuration of the setup. A relation between the measured value and the orientation of the handle is very unlikely and it seems to be a measurement error. Therefore, it is assumed that the handle of the coffee cup has no significant influence on the scattering properties of the coffee cup and the variation of the measured values are caused by the measurement equipment.

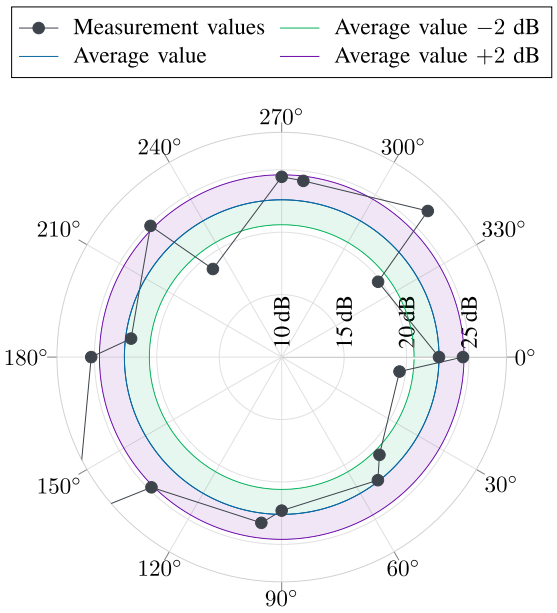

Fig. 7. Reflection loss of the coffee cup for different handle orientations φ_{handle}.

TABLE IV
PL INCLUDING THE FSPL FOR DIFFERENT LAPTOP SURFACE ORIENTATIONS

Surface orientation	45°	135°	225°	315°
PL	108.10 dB	131.09 dB	105.96 dB	127.91 dB

On the other hand, the reflection properties of the laptop are strongly depend on the orientation of the surface of the open laptop as shown by the results of the general characteristics in Section III-A. If the laptop is set with a 45° incident angle between the LOS path between Alice and Bob and the surface of the open laptop, it behaves like a mirror and reflects the scattered signal directly in the direction of Eve for a viewing angle of 90° (see Laptop 45° in Fig. 3). In this case, the minimal reflection loss is approximately 5 dB. To evaluate whether the texture of the surface has an influence on the reflection loss or not, the reflection for Laptop 45° is measured for four different orientations of the surface. Therefore, the laptop was placed at $x_{\text{scat}} = 2.5$ m and at $y_{\text{scat}} = 0$ m. Eve was placed at $x_{\text{Eve}} = 2.5$ m and the normal vector of the display was varied within the range of [45; 315]° in 90° steps with respect to φ.

The measured values, summarized in Table IV, reinforce the observations in Section III-A: the PL is smaller if the surface of the laptop is set in the direction of 45° and 225°. In these cases, the surface reacts as a mirror and reflects the transmitted signal directly into the direction of Eve. The values emphasize that the reflection loss is similar for the front and rear side of the laptop: for 45° the cover of the laptop is the mirror plane whereas the display is the mirror plane for 225°. However, the measured values have a gap of approximately 3 dB only. The same observations can be made for the other orientation where the gap is also approximately 3 dB but the PL is approximately 22 dB higher.

IV. SECURITY ASPECTS

In this section, the measurement results will be investigated with respect to the secrecy capacity (SC), starting with the theoretical background in the first part of this section. For Eve, the SC should be low while Alice and Bob should not notice the attack. Therefore, the blockage of Bob has to be considered, too, and will be investigated in the second part of this section. Finally, the SC for the different objects and positions is analyzed in the last part of this section.

A. Theory

The SC here is given by the normalized SC and can be calculated by [14]

$$\overline{c}_{\text{s}} = \frac{\log(1+\text{SNR}_{\text{Bob}}) - \log(1+\text{SNR}_{\text{Eve}})}{\log(1+\text{SNR}_{\text{Bob}})}. \tag{5}$$

The signal-to-noise ratio (SNR) for Bob and Eve can be calculated by

$$\text{SNR}_{\Omega} = 10^{\frac{\text{SNR}_{\Omega,\text{dB}}}{10}} \tag{6}$$

where Ω denotes Bob and Eve, respectively, and the logarithmic SNR is

$$\text{SNR}_{\Omega,\text{dB}} = P_{\Omega,\text{dBm}} - P_{\text{noise,dBm}}. \tag{7}$$

The received power $P_{\Omega,\text{dBm}}$ is given by

$$P_{\Omega,\text{dBm}} = P_{\text{TX,dBm}} + G_{\text{ant,TX,dBi}} - L_{\text{path},\Omega,\text{meas,dB}} + G_{\text{ant,RX,dBi}} \tag{8}$$

where $P_{\text{TX,dBm}}$ denotes the transmit power of Alice and is set to 10 dBm, $G_{\text{ant},\cdot}$ is the maximum antenna gain, and $L_{\text{path},\Omega,\text{meas,dB}}$ is the measured PL including the FSPL and the optional reflection loss at Bob or Eve, respectively. In contrast to (3), the difference in the PL due to the different antenna gains at different AODs is considered here because the SC shall be analyzed even if the scattering object receives a signal transmitted in direction of the side lobes of the antenna of Alice.

For the noise power, an additive white Gaussian noise (AWGN) channel with thermal noise is assumed and is given by

$$P_{\text{noise,dBm}} = 10 \cdot \log_{10}\left(\frac{\text{k}_{\text{B}} \cdot T \cdot B}{1\ \text{mW}}\right) + \text{NF} \tag{9}$$

where k_{B} is the Boltzmann's constant. The temperature T is assumed to be $T = 290$ K and according to the IEEE 802.15.3d standard the bandwidth B is set to $B = 2.16$ GHz. The noise figure NF is assumed with 8 dB [1].

B. Blockage of Bob

The blockage of Bob can be calculated by [14]

$$b = 1 - \frac{\text{SNR}^{\alpha}_{\text{Bob}}}{\text{SNR}^{\text{no object}}_{\text{Bob}}} \tag{10}$$

where the SNR is calculated following (6)–(9) and α denotes the investigated scattering object. If the scattering object is placed directly in the LOS path between Alice and Bob (each position where $y_{\text{scat}} = 0$ m), the blockage of Bob is between

TABLE V
BLOCKAGE OF BOB

x-Pos.	y-Pos.	Coffee Cup	Thermos	Laptop 45°	Laptop 90°
1.5 m	0.000 m	0.97	0.97	0.96	0.99
	0.105 m	0.13	0.09	0.07	0.00
	0.184 m	0.12	0.00	0.00	0.00
2.5 m	0.000 m	0.96	0.93	0.95	0.99
	0.175 m	0.14	0.00	0.00	0.00
	0.307 m	0.12	0.00	0.00	0.00
3.5 m	0.000 m	0.99	0.97	0.96	0.99
	0.245 m	0.10	0.00	0.00	0.00
	0.430 m	0.11	0.00	0.00	0.00

TABLE VI
AVERAGE SECRECY CAPACITY

Object	y-Position	x_{scat} 1.5 m	2.5 m	3.5 m
Coffee cup	LOS	0.18	0.44	0.39
	AOD 4°	0.48	0.68	0.75
	AOD 7°	0.60	0.80	0.87
Thermos	LOS	0.10	0.24	0.24
	AOD 4°	0.44	0.52	0.58
	AOD 7°	0.52	0.64	0.71
Laptop 45°	LOS	0.45	0.69	0.86
	AOD 4°	0.67	0.88	0.93
	AOD 7°	0.76	0.94	0.96
Laptop 90°	LOS	0.47	0.69	0.80
	AOD 4°	0.70	0.85	0.94
	AOD 7°	0.81	0.93	0.97

0.93 and 0.99. If the object is placed outside of the LOS path, the blockage of Bob is zero in most of the cases. The blockage is greater than zero (more precisely between 0.07 and 0.14) for the coffee cup, for one of the positions of the Thermos, and for one of the positions of the Laptop 45°. However, the receiving power of Bob is approximately 1 dB higher at those positions compared to the other positions. Due to the accuracy of the measurement system, it can be assumed that the receiving power is the same if the object is placed outside of the LOS path and therefore these blockage values can also be assumed to be zero. Thus, Alice and Bob only notice the attack if the scatterer is placed directly in the LOS path. The results of Bob's blockage are summarized in Table V.

C. Secrecy Capacity

As mentioned in the previous section, Alice and Bob will notice the attack due to the blockage which is higher than 0.93 if the objects were placed in the LOS path between Alice and Bob. However, given the placement in the LOS path, the SC is low for the coffee cup and the thermos if the scatterer is placed at $x_{\text{scat}} = 1.5$ m as shown in Fig. 8 as a blue dashed line with circular markers. The average values, summarized in Table VI, are 0.10 for the thermos and 0.18 for the coffee cup if the scatterer is placed at $x_{\text{scat}} = 1.5$ m. The SC is increased to 0.24 for the thermos and 0.44 for the coffee cup when the scatterer is placed at $x_{\text{scat}} = 2.5$ m, and to 0.24 for the thermos and 0.39 for the coffee cup with the scatterer at $x_{\text{scat}} = 3.5$ m. An SC of 0 is reached as the lowest value because Eve partially receives the same power as Bob due to the good reflection and the blockage of the scattering object. On the other hand, the SC is much higher if the laptop is used as the scattering object even if it is placed in the LOS path, except for the cases where the Laptop 45° reflects the signal in a specular way. The average values lie between 0.45 and 0.86 for Laptop 45° and between 0.47 and 0.80 for Laptop 90° if the object is placed in the LOS path.

As expected, the SC increases with increasing distance in y-direction of the scattering object because the received power decreases for Eve due to the higher PL whereas the received power concurrently increases for Bob due to the absent blockage. In Fig. 8, the different positions are shown as a purple dashed line with square markers for the scattering object position with an AOD of 4° and as a gray dashed line with triangle markers for the position with an AOD of 7°. However, the deviation of the SC between the two different positions outside the LOS–where the scattering object receives the signal from Alice with an AOD of 4° and 7°, respectively–is relatively small. The difference of the SC, i.e., the difference of the purple and gray dashed line for each position of Eve and for all sub-figures in Fig. 8, has a maximum of 0.23, a minimum of 0.08, and an average value of 0.09. This is independent of the scattering object itself, its x-position, and the position of Eve. Similar to the findings before, the SC for the coffee cup and for the thermos is lower and therefore the eavesdropping opportunities are better than for the laptop.

With respect to the laptop, the values are comparable for Laptop 45° and Laptop 90° expect for the configuration where the Laptop 45° reflects in a specular way. For the position where the scattering object receives the transmitted signal with an AOD of 4°, the average SC is 0.83 both for Laptop 45° and for Laptop 90° for all positions of the scattering object as well as for all positions of Eve. For the AOD of 7°, the average are 0.89 for Laptop 45° and 0.90 for Laptop 90°. It can be seen that the SC is greater than 0.6 in most of the cases here which makes eavesdropping difficult. This is especially true when the scatterer is placed at $x_{\text{scat}} = 2.5$ m and at $x_{\text{scat}} = 3.5$ m: here, the SC is even greater than 0.8 in most of the cases. Furthermore, the results show that "direct eavesdropping," i.e., Eve is directly aligned toward Alice and receives the transmitted signal via side lobes of Alice's antenna, might be more effective if the laptop is placed outside of the LOS path. The SC for the direct eavesdropping–visualized as a green solid reference line in Fig. 8–is lower than the SC for the reflected path for the predominant number of Eve's positions.

On the other hand, for the coffee cup and for the thermos most SC values are below 0.8 and 0.7, respectively, if the object is placed outside of the LOS path. The average value is 0.64 for the coffee cup and 0.51 for the thermos if the object

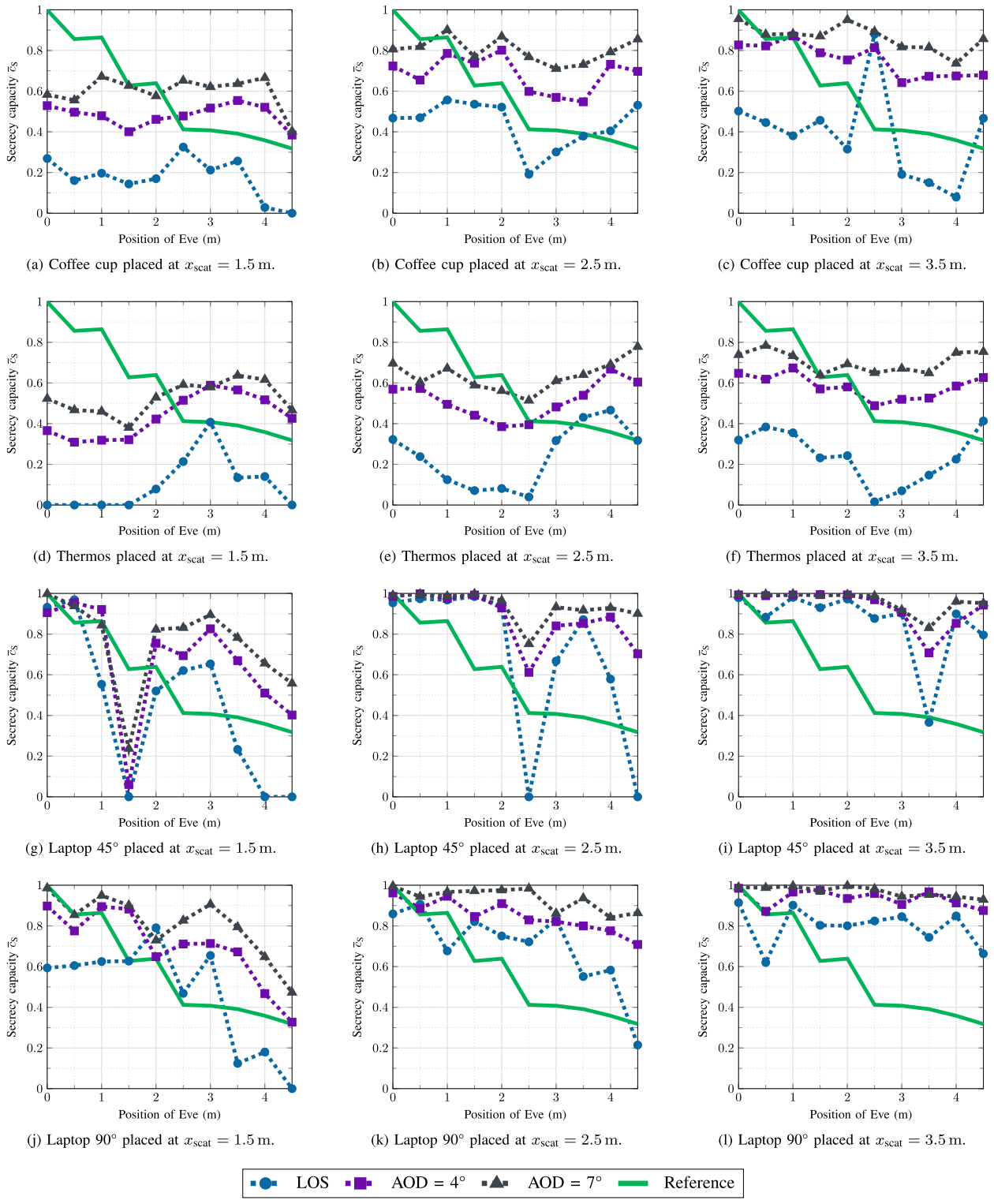

(a) Coffee cup placed at $x_{\text{scat}} = 1.5\,\text{m}$. (b) Coffee cup placed at $x_{\text{scat}} = 2.5\,\text{m}$. (c) Coffee cup placed at $x_{\text{scat}} = 3.5\,\text{m}$.

(d) Thermos placed at $x_{\text{scat}} = 1.5\,\text{m}$. (e) Thermos placed at $x_{\text{scat}} = 2.5\,\text{m}$. (f) Thermos placed at $x_{\text{scat}} = 3.5\,\text{m}$.

(g) Laptop 45° placed at $x_{\text{scat}} = 1.5\,\text{m}$. (h) Laptop 45° placed at $x_{\text{scat}} = 2.5\,\text{m}$. (i) Laptop 45° placed at $x_{\text{scat}} = 3.5\,\text{m}$.

(j) Laptop 90° placed at $x_{\text{scat}} = 1.5\,\text{m}$. (k) Laptop 90° placed at $x_{\text{scat}} = 2.5\,\text{m}$. (l) Laptop 90° placed at $x_{\text{scat}} = 3.5\,\text{m}$.

Fig. 8. SC for the different scattering objects at different positions based on the channel sounder measurements.

is placed in the direction of the AOD of 4° as well as 0.76 for the coffee cup and 0.62 for the thermos when the AOD of 7° is chosen. For the three different x-positions of the scattering object, the average SC for the thermos are 0.44, 0.52, and 0.58 for the AOD of 4° configuration as well as 0.52, 0.64, and 0.71 for the AOD of 7° configuration. The average values increase for the coffee cup: 0.48, 0.68, and 0.75 for the AOD of 4° configuration as well as 0.60, 0.80, and 0.87 for the AOD of 7° configuration.

With respect to direct eavesdropping, the SC is higher in two thirds of the positions of Eve if the coffee cup is placed at $x_{\text{scat}} = 2.5$ m and $x_{\text{scat}} = 3.5$ m outside of the LOS path.

Here, in most cases the direct eavesdropping might be more effective. If the thermos is used as a scattering object or the coffee cup is placed at $x_{\text{scat}} = 1.5$ m, eavesdropping via the reflection at the scattering object is more effective until Eve's position reaches approximately half of the way between Alice and Bob. Up to this point, the SC is lower compared to the SC when Eve is aligned directly toward Alice.

It should be noted that Eve is placed relatively close to Alice and Bob and to the LOS path between them here. On the one hand, this leads to similar FSPL values compared to the distance between Alice and Bob, but on the other hand this supports the direct eavesdropping as Eve can receive the signal from Alice via small AODs. If Eve is placed further away from the LOS between Alice and Bob, the SC of eavesdropping for the reflection at the scattering object might change slightly as the FSPL changes only a little. In contrast, the receiving power by means of direct eavesdropping will change more noticeable as the AOD changes. This means that the transmitted signal will be amplified with a lower antenna gain in this direction and that the benefit of the eavesdropping via the reflection at a scattering object might be stronger. On the other hand, the direct eavesdropping might be better if the transmitted signal benefits from strong side lobes in direction of Eve as can be observed by phased array antennas, for example [25].

V. Conclusion

Against the predominant opinion, previous work has shown that eavesdropping might be possible in THz communications even if high gain antennas are used. To complement these findings, eavesdropping opportunities with common objects in office-like scenarios, namely a coffee cup, a thermos, and a laptop, are evaluated in this article. Considering different positions of the scattering object, especially placed outside of the LOS path between Alice and Bob, channel sounder measurements were conducted to measure the receive power of Bob and Eve. In the end, details of the eavesdropping opportunities were investigated in form of scattering properties and SC.

With respect to the general scattering properties, the investigation reveals that the coffee cup and the thermos reflects better than the laptop whereby the thermos has the lowest reflection losses due to the material characteristics. For the coffee cup and the thermos, the results are independent of the filling or the temperature of the object. Furthermore, the reflection losses are independent of the orientation of the coffee cup and the thermos but they are strongly influenced by the orientation of the laptop. Therefore, the lowest reflection losses were measured for the laptop when it is oriented with an angle of 45° with respect to the LOS path between Alice and Bob as the laptop reflects in a specular way. The minimal measured reflection loss is approximately 5 dB in this case. In contrast, a first order approximation independent of the viewing angle of Eve leads to reflections losses of 26.9 dB for the coffee cup, 19.8 dB for the thermos, and 37.5 dB for the laptop if the surface of the laptop is oriented perpendicular to the LOS of Alice and Bob.

The SC should always be examined considering the blockage of Bob. The target of eavesdropping is a low SC together with a low blockage of Bob so that Alice and Bob do not notice the attack. The presented results show that the blockage of Bob is high with a minimum value of 0.93 if the scattering object is placed within the LOS between Alice and Bob. However, the blockage is always zero if the object is placed outside of the LOS, and therefore Alice and Bob will not notice the attack if the object is placed there. The SC is lower if the object is placed within the LOS, but even if the object is placed outside of the LOS, the SC is low using the thermos as a scattering object. For the thermos, the SC is always below 0.8. Compared to "direct eavesdropping" where Eve is directly oriented toward Alice, the SC of the direct eavesdropping is lower in the predominant number of cases compared to the SC when the signal is received in terms of reflection at the scattering object. Therefore, the results show that in the chosen setup the direct eavesdropping is more effective for Eve when other objects than the thermos are used as a scattering object. Especially if strong side lobes of, e.g., phased array antennas are considered, direct eavesdropping benefits of the side lobes and might be better than eavesdropping in terms of reflections.

It should be noted that the results regarding the SC depend on the position of Eve. If Eve is placed, for example, within a sidelobe of the antenna of Alice, the direct eavesdropping might be even better or, on the other hand, worse, if Eve is placed between two side lobes of the antenna of Alice. The dependency of the SC on the position of Eve extended to the variation of the y-position could be investigated in an ensuing work. Future work could also enhance the map predictions of office scenarios given in [10]. Here, the eavesdropping opportunities in terms of received power at Eve with respect to the position in a conference room were investigated. However, only the room itself with fixed objects, like TV screens and door frames, was considered. Based on the scattering properties evaluated in this work, the scenario could be complemented using freestanding objects, like the thermos or the laptop.

The different investigations of the physical layer security in low THz communications have shown that eavesdropping is possible in several ways: by means of reflections due to the room itself, by means of reflections of scattering objects within the room, and by means of the sidelobes of the antenna of Alice. Our measurement results and the evaluated SC are the basis for designing secure channel coding schemes using, for example, wiretap coding to enable a secure communication between Alice and Bob from an information-theoretical perspective.

References

[1] V. Petrov, T. Kürner, and I. Hosako, "IEEE 802.15.3d: First standardization efforts for sub-terahertz band communications toward 6G," *IEEE Commun. Mag.*, vol. 58, no. 11, pp. 28–33, Nov. 2020.

[2] *Attenuation by Atmospheric Gases and Related Effects*, International Telecommunication Union, Recommendation ITU-R P.676-13, 2022.

[3] *Attenuation Due to Clouds and Fog*, International Telecommunication Union, Recommendation ITU-R P.840-8, 2019.

[4] *Specific Attenuation Model for Rain for Use in Prediction Methods*, International Telecommunication Union, Recommendation ITU-R P.838-3, 2005.

[5] T. Kürner and S. Priebe, "Towards THz communications—Status in research, standardization and regulation," *J. Infr., Millim., Terahertz Waves*, vol. 35, no. 1, pp. 53–62, Jan. 2014.

[6] T. Schneider, A. Wiatrek, S. Preußler, M. Grigat, and R.-P. Braun, "Link budget analysis for terahertz fixed wireless links," *IEEE Trans. Terahertz Sci. Technol.*, vol. 2, no. 2, pp. 250–256, Mar. 2012.
[7] J. Federici and L. Moeller, "Review of terahertz and subterahertz wireless communications," *J. Appl. Phys.*, vol. 107, no. 11, 2010, Art. no. 111101.
[8] I. F. Akyildiz, J. M. Jornet, and C. Han, "Terahertz band: Next frontier for wireless communications," *Phys. Commun.*, vol. 12, pp. 16–32, Sep. 2014.
[9] S. Vuppala, S. Biswas, and T. Ratnarajah, "An analysis on secure communication in millimeter/micro-wave hybrid networks," *IEEE Trans. Commun.*, vol. 64, no. 8, pp. 3507–3519, Aug. 2016.
[10] C. Herold, T. Doeker, J. M. Eckhardt, and T. Kürner, "Investigation of eavesdropping opportunities in a meeting room scenario for THz communications," in *Proc. 16th Eur. Conf. Antennas Propag. (EuCAP)*, Madrid, Spain, Mar. 2022, pp. 1–5.
[11] R. Piesiewicz, C. Jansen, D. Mittleman, T. Kleine-Ostmann, M. Koch, and T. Kürner, "Scattering analysis for the modeling of THz communication systems," *IEEE Trans. Antennas Propag.*, vol. 55, no. 11, pp. 3002–3009, Nov. 2007.
[12] M. Jacob, S. Priebe, R. Dickhoff, T. Kleine-Ostmann, T. Schrader, and T. Kürner, "Diffraction in mm and sub-mm wave indoor propagation channels," *IEEE Trans. Microw. Theory Techn.*, vol. 60, no. 3, pp. 833–844, Mar. 2012.
[13] C. Jansen, R. Piesiewicz, D. Mittleman, T. Kürner, and M. Koch, "The impact of reflections from stratified building materials on the wave propagation in future indoor terahertz communication systems," *IEEE Trans. Antennas Propag.*, vol. 56, no. 5, pp. 1413–1419, May 2008.
[14] J. Ma et al., "Security and eavesdropping in terahertz wireless links," *Nature*, vol. 563, no. 7729, pp. 89–93, Nov. 2018.
[15] D. Steinmetzer, J. Chen, J. Classen, E. Knightly, and M. Hollick, "Eavesdropping with periscopes: Experimental security analysis of highly directional millimeter waves," in *Proc. IEEE Conf. Commun. Netw. Secur. (CNS)*, Florence, Italy, Sep. 2015, pp. 335–343.
[16] Y. Mei, Y. Ma, J. Ma, L. Moeller, and J. F. Federici, "Eavesdropping risk evaluation on terahertz wireless channels in atmospheric turbulence," *IEEE Access*, vol. 9, pp. 101916–101923, 2021.
[17] Z. Fang, H. Guerboukha, R. Shrestha, M. Hornbuckle, Y. Amarasinghe, and D. M. Mittleman, "Secure communication channels using atmosphere-limited line-of-sight terahertz links," *IEEE Trans. Terahertz Sci. Technol.*, vol. 12, no. 4, pp. 363–369, Jul. 2022.
[18] R. Shrestha, H. Guerboukha, Z. Fang, E. Knightly, and D. M. Mittleman, "Jamming a terahertz wireless link," *Nature Commun.*, vol. 13, no. 1, p. 3045, Jun. 2022.
[19] T. Kürner, D. M. Mittleman, and T. Nagatsuma, Eds., *THz Communications: Paving the Way Towards Wireless Tbps* (Springer Series in Optical Sciences). Cham, Switzerland: Springer, 2022, vol. 234.
[20] C. Herold, T. Doeker, and T. Kürner, "Measurements at 300 GHz in eavesdropping scenarios and first results," in *Proc. 5th Int. Workshop Mobile Terahertz Syst. (IWMTS)*, Duisburg, Germany, Jul. 2022, pp. 1–4.
[21] S. Rey, J. M. Eckhardt, B. Peng, K. Guan, and T. Kürner, "Channel sounding techniques for applications in THz communications: A first correlation based channel sounder for ultra-wideband dynamic channel measurements at 300 GHz," in *Proc. 9th Int. Congr. Ultra Modern Telecommun. Control Syst. Workshops (ICUMT)*, Munich, Germany, Nov. 2017, pp. 449–453.
[22] T. Doeker, J. M. Eckhardt, and T. Kürner, "Channel measurements and modeling for low terahertz communications in an aircraft cabin," *IEEE Trans. Antennas Propag.*, vol. 70, no. 11, pp. 10903–10916, Nov. 2022.
[23] J. M. Eckhardt, T. Doeker, and T. Kürner, "Indoor-to-outdoor path loss measurements in an aircraft for terahertz communications," in *Proc. IEEE 91st Veh. Technol. Conf. (VTC-Spring)*, Antwerp, Belgium, May 2020, pp. 1–5.
[24] M. Dawood Al-Dabbagh, T. Doeker, T. Kleine-Ostmann, T. Kürner, and D. Humphreys, "THz channel sounder and VNA verification measurement based over-the-air multipath artifact," in *Proc. 47th Int. Conf. Infr., Millim. Terahertz Waves (IRMMW-THz)*, Delft, The Netherlands, Aug. 2022, pp. 1–2.
[25] S. Rey, T. Merkle, A. Tessmann, and T. Kürner, "A phased array antenna with horn elements for 300 GHz communications," in *Proc. Int. Symp. Antennas Propag. (ISAP)*, Okinawa, Japan, Oct. 2016, pp. 122–123.

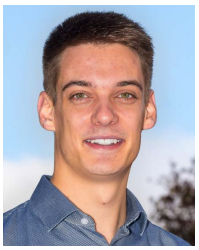

Tobias Doeker (Graduate Student Member, IEEE) was born in Haltern, Germany, in 1994. He received the Bachelor of Science (B.Sc.) degree in electrical engineering from the Hamburg University of Applied Sciences, Hamburg, Germany, in 2017, and the Master of Science (M.Sc.) degree in electrical engineering with a focus on communications technology from the Technische Universität Braunschweig, Braunschweig, Germany, in 2019, where he is currently pursuing the Ph.D. degree.

From 2013 to 2019, he was a Student Trainee at Lufthansa Technik AG, Hamburg. In November 2019, he joined the Institute for Communications Technology, Technische Universität Braunschweig, as a Researcher. His research interests are focused on THz communication and here especially on radio channel measurements and characterization as well as device discovery for multi gigabit indoor communication at 300 GHz.

Christoph Herold (Graduate Student Member, IEEE) was born in Lemgo, Germany, in 1990. He received the Bachelor of Science (B.Sc.) and Master of Science (M.Sc.) degrees in computer and communication systems design from the Technische Universität Braunschweig, Braunschweig, Germany, in 2016 and 2019, respectively, where he is currently pursuing the Ph.D. degree.

As a Researcher at the Institute for Communications Technology, Technische Universität Braunschweig. His research interests include the simulation of mobile communication systems on system- and link-level and the modeling of communication channels using ray tracing. He focuses on high data rate THz communication and its impact on secure communication in realistic scenarios.

Johannes M. Eckhardt (Graduate Student Member, IEEE) was born in Braunschweig, Germany, in 1992. He received the Dipl.-Ing. degree in electrical engineering from the Technische Universität Dresden, Dresden, Germany, in 2017, and the M.A. degree from École Centrale Paris, Paris, France, in 2017. He is currently pursuing the Ph.D. degree at the Department of Mobile Radio Systems, Institute for Communications Technology, Technische Universität Braunschweig, Braunschweig. His research interests include channel measurements and modeling, link-level simulations, and interference studies in complex scenarios for multi gigabit communication systems at THz frequencies.

Thomas Kürner (Fellow, IEEE) received the Dipl.-Ing. degree in electrical engineering and the Dr.-Ing. degree from the University of Karlsruhe, Karlsruhe, Germany, in 1990 and 1993, respectively.

From 1990 to 1994, he was with the Institut für Höchstfrequenztechnik und Elektronik (IHE), University of Karlsruhe, working on wave propagation modeling, radio channel characterization, and radio network planning. From 1994 to 2003, he was with the Radio Network Planning Department at the headquarters of the GSM 1800 and UMTS operator E-Plus Mobilfunk GmbH & Co KG, Düsseldorf, Germany, where he was the Team Manager Radio Network Planning Support responsible for radio network planning tools, algorithms, processes, and parameters, from 1999 to 2003. Since 2003, he has been a Full University Professor for mobile radio systems at the Technische Universität Braunschweig, Braunschweig, Germany. In 2012, he was a Guest Lecturer at Dublin City University, Dublin, Ireland, within the Telecommunications Graduate Initiative in Ireland. He was the Project Coordinator of the H2020-EU-Japan Project ThoR ("TeraHertz end-to-end wireless systems supporting ultrahigh data Rate applications") and the Coordinator of the German DFG-Research Unit FOR 2863 Meteracom ("Metrology for THz Communications").

From 2016 to 2021, he was a member of the Board of Directors of the European Association on Antennas and Propagation (EurAAP). From 2020 to 2022, he was a Distinguished Lecturer of IEEE Vehicular Technology Society. In 2019 and 2022, he received the Neal-Shephard Award of the IEEE Vehicular Technology Society (VTS). Currently, he is chairing the IEEE 802.15 Standing Committee THz. He was the Chair of IEEE 802.15.3d TG 100G, which developed the worldwide first wireless communications standard operating at 300 GHz.